Image Enhancement and Understanding for Remote Visual Inspection of Aircraft Surface.

Priyan Gunatilake[*], M.W. Siegel[**], A.J. Jordan[*,**], G. Podnar[**]

[*]Department of Electrical and Computer Engineering
[**]Robotics Institute, School of Computer Science
Carnegie Mellon University
Pittsburgh, PA.

ABSTRACT

We describe a library of image enhancement and understanding algorithms developed to enhance and recognize surface defects from remote live imagery of an aircraft surface. Also described are the supporting mobile robot platform that generates the remote stereoscopic imagery and the inspection console containing a graphical user interface, through which the inspector accesses the live imagery for remote inspection. We will discuss initial results of the remote imaging process and the image processing library, and speculate on their future application in aircraft inspection.

Keywords: ANDI, CIMP, aircraft visual inspection, remote visual inspection, image enhancement, image understanding, stereo vision

1. Introduction

Visual inspection is, by far, the most widely used method in aircraft surface inspection.[1] However, the current practice of getting on the aircraft body to carry out inspection raises safety issues for the inspector, is time consuming, and suffers at times from being ineffective due to inspector fatigue or boredom.[2] Enhanced remote visual inspection could allow the inspector to safely, quickly and accurately perform the necessary visual inspection. We are currently developing a prototype aircraft-capable mobile robot called the Crown Inspection Mobile Platform (CIMP). CIMP relays high quality, live stereoscopic imagery of the aircraft crown to an inspection console manned by the inspector. The inspector, with the aid of computer enhancement and intelligence, examines the imagery for surface defects.

In this paper, we will describe several image enhancement algorithms, and an inspector's interface for accessing them, for highlighting surface cracks, scratches, lightning strikes and corrosion in the live imagery. Image enhancement algorithms emphasizes image features that are characteristic of surface defects such as cracks and corrosion. We will also describe some experiments with an image understanding algorithm that use 2D and 3D features extracted from live imagery combined with an active vision sensor developed in our laboratory. Image understanding algorithms may, in the foreseeable future, make it feasible to automate screening of large volumes of image data so that inspectors can concentrate on imagery suggestive of anomalies; in the more distant future, ongoing progress may permit an even greater degree of machine assistance and automation for visual detection of surface cracks and corrosion.

Image enhancement and understanding algorithms are already extensively used with great success in medical imaging applications, and we believe that they could make a similar impact in the area of aircraft surface

inspection.

1.1   Background

The **A**utomated **N**on-**D**estructive **I**nspection (ANDI) robot, developed at Carnegie Mellon University, success-fully demonstrated mobility, manipulation and navigational capabilities of a robot on an aircraft surface. [3,4] ANDI carried a sensor package consisting of an eddy current probe and four cameras for remote navigation. The cameras were useful for observing gross visual features, but not of optical or electronic quality suitable for detailed visual inspection. However, due to the emphasis on mobility and navigation, the issue of accumulating useful inspection data was not addressed at length. After the initial demonstration of ANDI, the second author launched another research effort with the twin objectives of designing a sensor package for CIMP that would generate useful inspection data, and developing a graphical user interface (GUI) and a library of image enhancement and understanding algorithms, through which an inspector could access, enhance and recognize surface defects from live imagery. Figures 1 and 2   show the ANDI and CIMP robots.
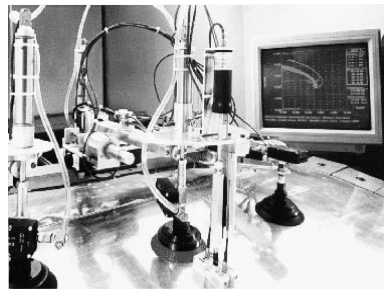

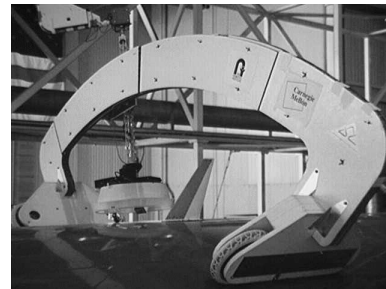Figure 1   ANDI on a section of aircraft surface in our laboratory.

Figure 2. CIMP on the crown of a Boeing 747, at Northwest's Minneapolis 747 maintenance facility

CIMP is designed to facilitate the development and testing of the remote imaging process and the capabilities of the library of image processing algorithms. Evaluations from extensive field testing will determine if the above system is acceptable to the aircraft inspectors, so that they are comfortable and willing to perform inspection remotely and thus realize its benefits. If successful, a logical next step would be to build an aircraft-capable, mobile inspection robot. This robot would be based on the marriage of technologies developed for mobility and navigation with ANDI and sensor, inspection workstation design and image processing algorithms developed with CIMP. However, if non-technical factors such as cost and inspector reluctance rule out a mobile inspection robot for the immediate future, the core sensor and image processing technologies developed with CIMP could still be applied to new products such as a hand-held video imaging unit with heads-up display for difficult or hazardous area visual inspection (for example, fuel tanks and aircraft interior panels) or to existing technologies such as video boroscopic, x-ray and MOI image interpretation.

1.2 Paper Outline

Section 2. describes the CIMP sensor package consisting of a pair of stereoscopic cameras and dynamic lighting controlled remotely by the inspector. The hardware and software components of the inspection console

through which the inspector accesses the remote imagery is described in Section 3. Three monoscopic and two stereoscopic image enhancement algorithms are described in Section 4. Section 5. details our current work in algorithm development on image understanding. Section 6. discusses recent results of field trials of CIMP on a Boeing 747 aircraft, at Northwest Airlines maintenance and inspection hangers in Minneapolis. Section 7. is the conclusion.

2.0 Sensor Package

A typical heavy inspection check is about 90% visual and 10% NDI.[1] With this in mind, the CIMP sensor package was designed to carry initially remote vision cameras and lighting equipment, with options later to add NDI equipment. The sensor package contains a stereoscopic pair of inspection cameras, a dynamic lighting array consisting of two fixed flood lights and a rotatable directional light source, and a pair of proprioceptive navigational cameras. The inspection cameras provide narrow-angle, 3.5X magnified, high quality imagery of the aircraft surface. These cameras were developed in our laboratory, and are constructed in a geometrically correct imaging configuration that provides natural, easy to view, high quality stereoscopic imagery of the aircraft surface.[5,6] The navigational and proprioceptive cameras provide a wide-angle stereoscopic view of CIMP with respect to the aircraft body that is used by the inspector to control and navigate CIMP. The left and right streams of the inspection and navigational cameras are interleaved at 120 Hz on a monitor, and viewed stereoscopically through active eyeware that will be described in section 3. The design of the rotatable directional light source was motivated by our observation of a test for surface crack detection, practiced widely by current inspectors. In this test, the inspectors observe the reflection of directional lighting produced by a flashlight held at a low angle to the surface Lack of reflecting light indicates the possibility of a presence of a crack. With the inclusion of the rotatable directional light source, our preliminary experiments indicate an inspector can successfully perform the surface crack detection test remotely through CIMP.

3.0 Inspection Console

3.1 Hardware

CIMP's motion, lighting array residing in the sensor package, and switching between the inspection and the navigational cameras are controlled by the inspector through a hand held remote-control unit. The current inspection console consists of two primary displays and their supporting equipment. The first is a monitor that provides live, flicker-free, full spatial and temporal resolution per eye, stereoscopic imagery of either the inspection or navigational camera pair. The second is a Silicon Graphics Indy workstation with a GUI (to be described shortly) that displays a single channel of the selected camera pair and is also an interface to the image processing algorithms. Our current ability to display only live monoscopic video imagery on the GUI is a limitation of the Indy workstation; similar but more powerful (and more expensive) workstations in the same family can display full motion stereoscopic imagery.

3.2 Software

We have developed a GUI called the Intelligent Inspection Window (IIW). The IIW performs a variety of functions: it displays live monoscopic or still stereoscopic video imagery on a part of its canvas called the display screen; it acts as the operational interface and output display unit to the image enhancement and understanding algorithms that are tied to menus and buttons on the IIW; and in the future, it will contain facilities for creating, editing, storing and retrieving facilities for multimedia record keeping of surface defects. Figure 3 shows the IIW.

Figure 3. Intelligent Inspection Window (IIW)

4.0 Image Enhancement

Image enhancement algorithms consist of a set of fast monoscopic and stereoscopic algorithms which, when applied to the live video imagery, highlight surface features such as scratches, cracks, lightning strikes and corrosion. The extent of highlighting is controlled by the inspector via a sensitivity parameter, represented in the IIW by a slidebar. By placing the sensitivity parameter under user control, we allow the inspector to experiment with a wide range of enhancement strengths which helps in discriminating surface defect features from normal features.

4.1 Monoscopic Image Enhancement
Monoscopic enhancement algorithms highlight features on the current live image displayed on the display screen of the IIW. We describe three monoscopic image enhancement methods that are now fully implemented on the IIW.

4.2.1 High-Frequency Emphasis

High-frequency emphasis involves a high-pass spatial filtering operation followed by adding of a fraction of the low-frequency components back to the filtered image. The gain of the high-pass filter is controlled by the sensitivity parameter under the inspector's control. This method is quite useful in highlighting scratches, cracks and corrosion texture, since these defects are of high frequency nature. Figures 4 displays a live image and an image with a mild degree of high-frequency emphasis. Note the appearance of lines on the enhanced

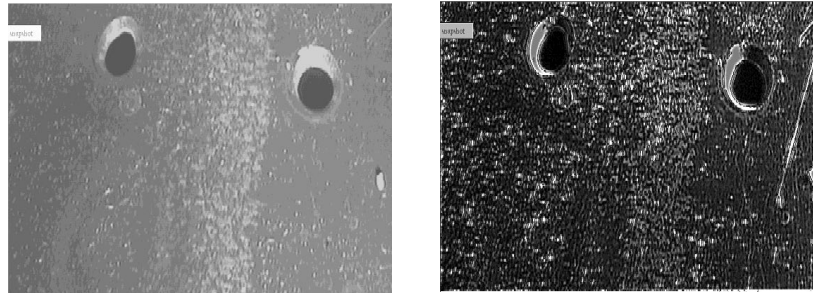images,   calling attention to scratches and cracks.

Figure 4. Live image of an inspection surface (left) and its high-frequency emphasized image (right).
Cracks, scratches and texture are highlighted in high-frequency emphasis operation.

Many live images suffer from low contrast due to lack of inherent detail exacerbated by excessively diffuse lighting. Thus defective areas such as scratches, cracks and corrosion texturing are almost invisible to the naked eye. These features are often not particularly highlighted by the high-frequency emphasis algorithm. Performing a histogram equalization[1] operation prior to the high-frequency emphasis increases the chances of highlighting such defective areas of the input image. Figure 5 displays a live low contrast image and a histogram equalized, high-frequency emphasis image. Note the appearance of scratches that are near invisible in the live image.
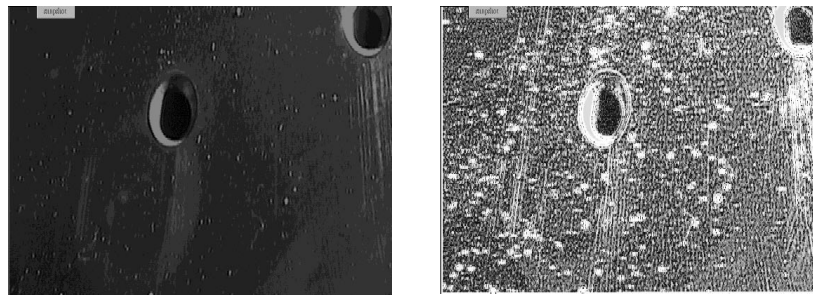

Figure 5. Live image of a low contrast inspection surface (left) and its histogram equalized, high-frequency emphasized image (right). Features that are near invisible in the low contrast image are highlighted in the histogram equalized, high-frequency emphasis operation

4.1.2 Sharpening by Differentiation

Sharpening performs an edge detection operation on the input image. We use a stochastic gradient filter convolved with the input image to generate the edge image. Edges are identified in the filtered image by thresholding the absolute value at each pixel. A variable threshold algorithm determines the threshold value based on the value of the GUI sensitivity slidebar and the statistics of the image intensity histogram.

1. A "low contrast" image is one that fails to match the sensitivity and dynamic range of the image capture and display medium to the level and range of gray levels actually present in the scene. The histogram equalization algorithm remaps the initial set of gray levels to a new set in which each gray level from full black to full white is equally probable, i.e., the histogram of gray levels is "equalized", or made flat. In practice the relatively small number of intensity quantization levels in the original image, typically only 256, of which even fewer are actually utilized in typical low contrast images, makes it impossible to achieve an exactly flat histogram.[7]
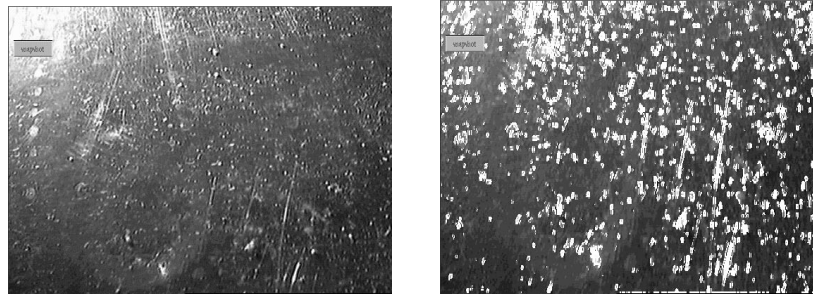
Figure 6 shows a live image and a sharpened image.

Figure 6. Live image of an inspection surface (left) and its sharpened image (right). Cracks and scratches
are highlighted in the sharpened image.

4.1.3 Adaptive Histogram Equalization

Global histogram modification schemes such as histogram equalization, transforms image pixels based on
overall image statistics. However, it is often necessary to enhance detail over a smaller area (for example, in a
rectangle containing a small crack). Frequently this local enhancement is not accomplished via a global histo-
gram equalization scheme. This is because the total number of pixels in such an area is small and has little
impact on the global statistics that drive the latter transformation. The solution to this problem offered by the
adaptive histogram equalization scheme, is to devise transformation functions that are based on pixel intensity
statistics in the neighborhood of each pixel in the live image.

Therefore adaptive histogram equalization involves selecting a local neighborhood centered around each pixel,
calculating and equalizing the histogram of the neighborhood, and then mapping the centered pixel based on
the new equalized local histogram. Keeping with our philosophy of providing adaptive control of enhancement
algorithms to the inspector, we have tied the sensitivity slidebar to the size of the local neighborhood window.
Thus, selecting a high sensitivity rating generates a smaller window size (minimum 4 x 4 pixels) and is sensi-
tive to small detail, while a lower sensitivity rating generates a larger window size (maximum 16 x 16) and is
sensitive to larger detail. Figure 7 shows adaptive histogram equalization with window size 4 x 4.
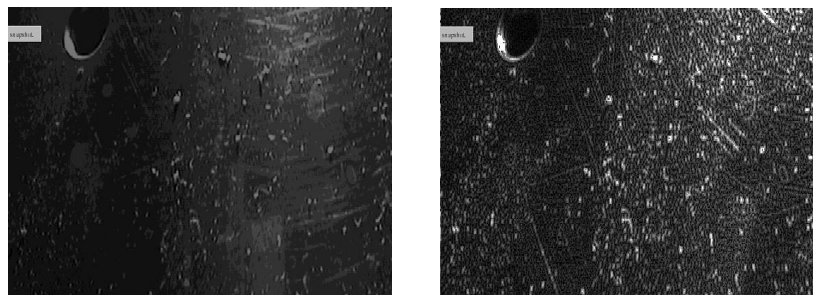

Figure 7. Live image of low contrast inspection surface (left) and its adaptive histogram equalized image
(right) of size 4 x 4 pixels. Note the appearance of scratches and fine texture in the enhanced image.

4.2 Stereoscopic Image Enhancement

We have implemented two stereoscopic image enhancement methods on the IIW. They are:

- Stereoscopic high-frequency emphasis

- Augmented-stereoscopic high-frequency emphasis (an artificial exaggeration of the inherent stereo-scopic information content)

These algorithms sample the input video sources to capture the left and right images corresponding to the current image displayed on the IIW. The captured images are processed individually by the specified algorithm and displayed on the IIW display screen. The inspector views this screen stereoscopically through the active eyeware that is synchronized with the display. We have included in the IIW, two slidebars that control the horizontal and vertical disparities[2] between the displayed left and right frames. The inspector, by adjusting these slidebars to a desired level, can comfortably view the displayed frames stereoscopically.

4.2.1 Stereoscopic high-frequency emphasis

The stereoscopic high-frequency emphasis algorithm consists of a histogram equalization followed by a high-frequency emphasis operation on the left and right input frames respectively. The resulting output frames are displayed on the IIW display. Histogram equalization is performed prior to high-frequency emphasis in order to approximately normalize the intensity distribution of the left and right frames, that may be different due to varying lighting conditions, apertures etc. between the two physical cameras. Figure 8 shows the left and right stereoscopic high-frequency emphasized images. Note that some features highlighted on one image is not present in the other image. This can be due to occlusion or different intensity distributions despite the histogram equalization step. When viewing a scene containing these singular features stereoscopically, they draw the inspector's attention due to their difficulty in fusing.
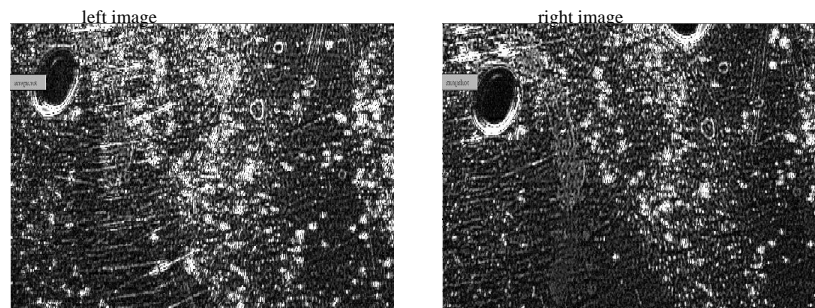

Figure 8. left and right high-frequency emphasized images. These images are viewed stereoscopically by the inspector.

2. Vertical disparity results from imperfect matching and alignment of the left and right cameras. It can be removed globally by digital relative up-down displacement of the two images. It must be removed because the optical axes of the human eyes are constrained by their neuromuscular control and actuation system more-or-less to a plane. Horizontal disparity is the result of the left-right offset between the camera axes. It is responsible for the perception of depth via the sense of "binocular stereopsis", and is thus desired and required. However excessively large horizontal disparities may be outside the range that the eye-brain system can handle comfortably. Reducing the mean value of the horizontal disparity distribution (by shifting) and/or compressing their range (by scaling) can make otherwise unviewable images viewable, and can make viewable images more pleasantly viewable. [8]

Thus, unexpectedly, these singular features along with the matched features, that represent the high-frequency content of the left and right frames, are brought to the attention of the inspector by the stereoscopic high-frequency emphasis algorithm.

4.2.2 Augmented-stereoscopic high-frequency emphasis

Augmented-stereoscopic imagery can be described as exaggerated stereoscopic imagery of a natural stereoscopic pair, realized by altering the natural disparity vector field. Augmented-stereoscopic imagery can be a powerful visualization technique since it can make features stand out with respect to the background by changing the relevant disparity maps in a complex scene. The augmented-stereoscopic high-frequency emphasis algorithm consists of four functional steps. The first two steps are similar to those of the stereoscopic high-frequency emphasis algorithm, where the left and right frames are histogram equalized and run through a high-frequency emphasis routine to locate the high frequency content. During the third step, the resulting left and right high-pass filtered frames are thresholded to generate the left and right binary feature maps. In the final step, the feature maps are overlaid with an offset that controls the extent of stereoscopic exaggeration (amount of disparity vector change), on the original left and right frames. Figure 9 show the original left and right images with overlaid corresponding feature maps. Note the change in spatial locations of noticeable features in the images (for example, edges of rivet outlines and scratches). The final left and right overlaid images are displayed on the IIW display. Augmented-stereoscopic high-frequency emphasized images display prominent high-frequency features such as scratches, cracks, texture etc. in a depth plane different from that of the background (aircraft surface) on the stereoscopic screen, making them more noticeable to the inspector. This differs from stereoscopic high-frequency emphasized images where high-frequency features and the background are essentially displayed on the same depth plane. However, augmented-stereoscopic high-frequency emphasis, like stereoscopic high-frequency emphasis, suffers from singular features caused by occlusion and intensity distribution mismatches between the original frames. Work on an algorithm that identifies singular features based on matching between left and right image features is underway. This algorithm could be used to filter out the singular features, so that stereoview of the above output images from the two algorithms is more comfortable to the inspector.

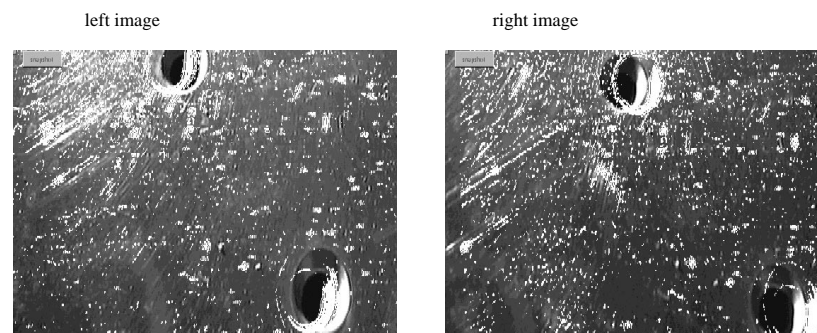left image   right image

Figure 9. The left and right augmented-stereo high-frequency emphasized images. Features are highlighted. Note the displacement of highlighted features in the images to produce the augmented-stereoscopic effect. For example, the outlines of the rivet heads are shifted from their natural locations. These images are viewed stereoscopically and the highlighted features appear in a different depth plane than the background (although physically they are on the same plane)

5. Image Understanding

Enhancement algorithms emphasize image features such as spatial high frequencies. Since aircraft surface defects such as cracks and surface corrosion are inherently of a high frequency nature, applying enhancement algorithms to imagery results in these defects being highlighted. However, also included in the set of emphasized features are normal features such as scratches, rivet heads, paint cracks and transitions, discoloration, dirt etc. due to their high frequency nature. Hence, it is left to the inspector's judgement, a function of talent and experience, to separate the skin defects from the normal features. The goal of image understanding algorithms is to combine to some extent, the image enhancement and the complex human interpretation process into a single program module. The recognition capability for surface flaws by an image understanding algorithm is achieved by correlating enhanced features of live imagery with a prior or learned knowledge of material flaws. However, developing a successful image understanding algorithm remains a rather difficult research challenge due to its dependence on many factors such as algorithm architecture, defect and normal feature characterization, a priori knowledge, learning and testing environments etc.

One possible scenario for application of image understanding algorithms is screening large volumes of image data. The image understanding algorithm can conservatively label all plausible defects, so that the inspector separates a larger fraction of actual defects from normal features in a smaller volume of raw data. Another scenario is the interactive use of these algorithms by inspectors to obtain a second opinion about a particular suspicious feature. The latter possibility is most attractive when the real-time inspector is relatively inexperienced, in general or with respect to a specific problem, compared to the inspector or inspectors whose expertise has been incorporated (explicitly or implictly) in the algorithm; in this case the computer fulfills a training role in addition to its direct inspection role.

5.1 Current work in Image Understanding Algorithms

Aircraft surface defects are characterized by their 2D and 3D features. For example, surface corrosion exhibits texture which is prominent as a 2D feature, whereas a surface dent or an area with subsurface corrosion creates a change in local surface curvature that is prominent as a 3D feature. A comprehensive image understanding algorithm needs to consider both types of features in its analysis and recognition of surface defects. Our image understanding algorithm extracts 2D and 3D features from the combination of live imagery that is displayed on the IIW and a range map generated by an active vision sensor.

We extract 2D edges and texture from the live imagery using a multiresolution, multiorientation wavelet framework. Edges are interesting features since they point to potential surface cracks, critical scratches and broken rivets. Texture is an interesting feature due to its high correlation with subsurface corrosion, lightning strikes etc. Unfortunately, live imagery contains countless number of edges and textures caused by simple scratches, lighting, repair patches, rivets etc. The challenge is thus to separate the interesting edges and texture

suggestive of defects from the rest. We achieve this within our wavelet framework by evaluating the strength of such features along the resolution axis. By arguing, that in general, image cracks are localized (tiny) and extend outwards from rivets, we are able to separate edges suggestive of cracks from normal edges (scratches, rivet head outlines etc.). Figures 10 -12 illustrates a section of aircraft surface, normal edges found by running our algorithm on the initial image and reduced pool of edges that may contain cracks. Note that the normal edges contain the outlines of rivet heads, scratches and a paint change. Similar work for recognition of texture indicative of corrosion is currently underway. The ability to discriminate features into probable defective features and normal features is important because it drastically reduces the feature pool that needs to be further processed to identify surface defects.
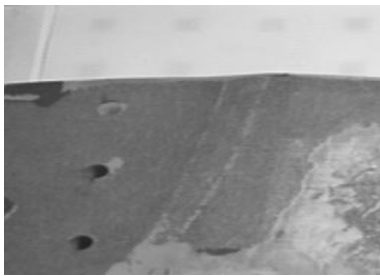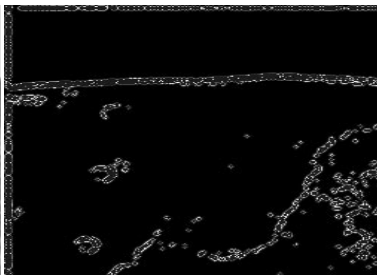
Figure 10. Live inspection surface

Figure 11. Normal edges detected from the live inspection surface. These edges correspond to rivet heads, scratches and paint transitions
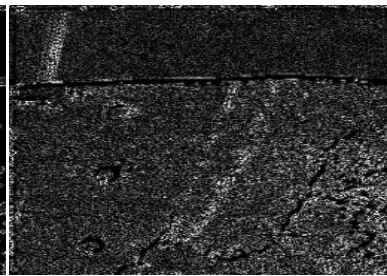
Figure 12. Reduced pool of edges that may contain possible cracks.

We extract 3D features from a range image created by an active vision sensor that was developed in our laboratory. The active vision sensor, which will be integrated into the sensor package of CIMP, employs a structured light laser source that is used in conjunction with the stereoscopic cameras to build a dense range map of depth accuracy of 0.5mm. The feature extraction from the range map generates a pool of areas of the imaged surface suggestive of pillowing, an indication of corrosion. Figures 13 and 14 illustrates the intensity (bright dots are laser spots) and range images of a part of an imaged surface. Note the bumps and dents on the range map, which appear exaggerated due to the artificial scale of the depth axis. Given a manufacturer's specification for allowable pillowing, these features could be used to identify and mark suspect areas.
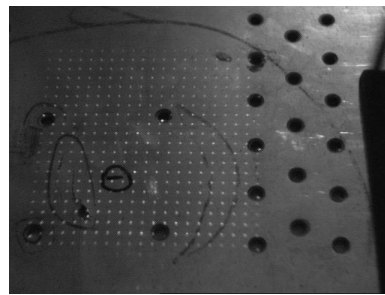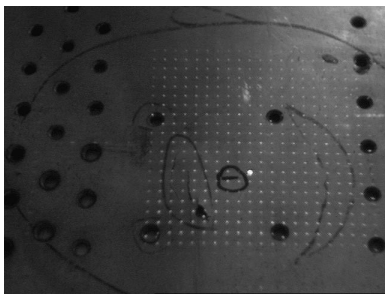
Figure 13. Left and right images of the inspection surface. The profiling laser spots of the active vision sensor are the bright spots seen in the images
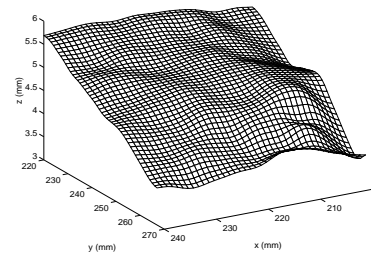
Figure 14. range map of the inspection surface Sample area indicated by laser spots in Fig 18 and 19.

The last component of our image understanding algorithm, currently under development, is a decision module

that binds the 2D and 3D feature extraction and analysis algorithms. This module takes a feature pool suggestive of defects generated by the separate 2D and 3D feature extraction and analysis routines described above, and uses its a priori and learned knowledge to recognize surface defects.

6. Field Results of CIMP

We have very successfully demonstrated CIMP's remote imaging capability to Northwest Airlines, USAir and US Air Force NDI Program Office, in our lab and at Northwest's Minneapolis 747 maintenance and inspection facility. The IIW and the library of image enhancement and understanding algorithms were not part of the demonstration at Northwest, since they are still under early development. Our demonstration proved that state-of-the-art 3D stereoscopic video technology, expertly implemented by us and operated by inspectors not specifically trained in its use, delivers imagery of sufficiently high visual quality that aircraft inspectors and NDI supervisors will accept it (and sometimes prefer it) as an alternative to direct visual inspection. Discussions with aircraft inspectors and NDI supervisors strongly indicate that they consider image enhancement for increased visibility of flaws to be valuable. However, they are skeptical about the feasibility of automated flaw detection through image understanding algorithms, but consider it a worthwhile research goal.

7. Conclusion

Our research efforts are directed at testing the hypothesized feasibility and advantages of remote visual inspection of aircraft surfaces. To test this premise, we have built CIMP, a prototype mobile robot that carries a remote imaging system, designed a GUI based inspection console, and are developing a library of image enhancement and understanding algorithms that together support remote visual inspection. Through field testing, we have demonstrated successfully that our remote live stereoscopic system delivers imagery of sufficiently high visual quality that aircraft inspectors are willing to accept it as an alternative to direct visual inspection. In this paper, we describe our efforts in the development of image enhancement and understanding algorithms. We believe that cooperative inspection involving men and computers working together, where application of these algorithms could be an early example, could contribute significantly to improving probability of flaw detection (POD), minimum detectable anomaly (MDA), and other quantitative and qualitative measures of successful and productive inspection activity.

8. Acknowledgment

9. References

1. I. L. Davis and M. W. Siegel, "Automated Nondestructive Inspector of Aging Aircraft",*International Symposium on Measurement Technology and Intelligent Instruments*, Huazhong University of Science and Technology, Wuhan, Hubei Province, People's Republic of China, October 1993.

2. W. T. Shepherd, "Human factors in aircraft maintenance and inspection", *Conference on aging aircraft and structural airworthiness*, NASA conference Publication 3160, pp 301-304, 1991.

3. M. W. Siegel, "Automation for Nondestructive Inspection of Aircraft", *Conference on Intelligent Robots in Field, Factory, Service and Space (CIRFFSS'94)*, Paul J Weitz (NASA/JSC), ed., AIAA, AIAA/NASA, pp. 367 - 377, Houston TX, March 1994.

4. M. W. Siegel, W. M. Kaufman, C. J. Alberts, "Mobile Robots for Difficult Measurements in Difficult Environments: Application to Aging Aircraft Inspection", Robotics and Autonomous Systems, Vol. 11, pp 187 - 194, July 1993.

5. V. S. Grinberg, G. W. Podnar, and M. W. Siegel, "Geometry of Binocular Imaging", *Proceedings of the SPIE/IST Conference (San Jose)*, ed., SPIE/IST, SPIE/IST, February 1994.

6. V. S. Grinberg, G. W. Podnar, and M. W. Siegel, "Geometry of Binocular Imaging ll: The Augmented Eye", *Proceedings of the SPIE/IST Conference (San Jose)*, ed., SPIE/IST, SPIE/IST, February 1995.

7. R. C. Gonzalez and P. Wintz, *Digital Image Processing*, Second Edition, Addison-Wesley, 1987.

8. J. S. McVeigh, M. W. Siegel and A. G. Jordan, "Algorithm for automated eye strain reduction in real stereoscopic images and sequences", *Proceedings of the SPIE/IST Conference (San Jose)*, ed., SPIE/IST, SPIE/IST, February 1996.